Available online at www.sciencedirect.com
ScienceDirect
Journal of Sound and Vibration 318 (2008) 364–388
JOURNAL OF SOUND AND VIBRATION
www.elsevier.com/locate/jsvi

Dynamic stiffness matrix of thin-walled composite I-beam with symmetric and arbitrary laminations

Nam-Il Kim, Dong Ku Shin*, Young-Suk Park

Department of Civil and Environmental Engineering, Myongji University, San 38-2, Nam-Dong, Yongin, Kyonggi-Do 449-728, Republic of Korea

Received 6 March 2007; received in revised form 1 April 2008; accepted 3 April 2008
Handling Editor: L.G. Tham
Available online 3 June 2008

Abstract

For the spatially coupled free vibration analysis of thin-walled composite I-beam with symmetric and arbitrary laminations, the exact dynamic stiffness matrix based on the solution of the simultaneous ordinary differential equations is presented. For this, a general theory for the vibration analysis of composite beam with arbitrary lamination including the restrained warping torsion is developed by introducing Vlasov's assumption. Next, the equations of motion and force–displacement relationships are derived from the energy principle and the first order of transformed simultaneous differential equations are constructed by using the displacement state vector consisting of 14 displacement parameters. Then explicit expressions for displacement parameters are derived and the exact dynamic stiffness matrix is determined using force–displacement relationships. In addition, the finite-element (FE) procedure based on Hermitian interpolation polynomials is developed. To verify the validity and the accuracy of this study, the numerical solutions are presented and compared with analytical solutions, the results from available references and the FE analysis using the thin-walled Hermitian beam elements. Particular emphasis is given in showing the phenomenon of vibrational mode change, the effects of increase of the modulus and the bending–twisting coupling stiffness for beams with various boundary conditions.

1. Introduction

Thin-walled beams made of anisotropic materials have increased in use in many civil, mechanical and aerospace engineering applications because of the high strength-to-weight and stiffness-to-weight ratios and their ability to be tailored to meet the design requirements of stiffness and strength. Other advantages that motivate some applications are corrosion resistance, magnetic transparency, low thermal expansion, and excellent fatigue characteristics in the direction of the fibers. For any structure that may be subjected to dynamic loads, the determination of the natural frequencies is critical in the design process. It is usually the first step in a dynamic analysis since a great deal may be deduced concerning the structural behavior and integrity from the knowledge of its natural frequencies and mode shapes.

*Corresponding author.
E-mail address: dkshin@mju.ac.kr (D.K. Shin).

0022-460X/$ - see front matter © 2008 Published by Elsevier Ltd.
doi:10.1016/j.jsv.2008.04.006

Up to the present, for the free vibration analysis of composite beams, the finite-element (FE) method has been widely used because of its versatility and a large amount of work [1–13] was devoted to the improvement of composite finite elements in order to obtain the acceptable results. Piovan and Cortínez [1] developed a new theoretical model for the free vibration, static, and buckling analyses of anisotropic open and closed cross-section composite thin-walled beams with general stacking sequences and arbitrary states of initial stresses and off-axis loadings. They took into account, in a full form, the shear flexibility due to bending and warping and introduced a non-shear-locking 7 dof per a node to validate their model. Lee and Kim [2] developed a displacement-based one-dimensional (1D) FE model to predict natural frequencies and corresponding vibration modes for a thin-walled composite I-beam. Through numerical results, they addressed the effects of fiber angle, modulus ratio, height-to-thickness ratio, and boundary conditions on the vibration frequencies of composite beam. Three higher-order displacement modes have been proposed and tested by Marur and Kant [3] for free vibration analysis of composite beams with various boundary conditions and aspect ratios using the FE modeling based on isoparametric formulations. The free vibration characteristics of laminated composite beams using the FE analysis and the higher-order plate theory was studied by Chandrashekhara and Bangera [4]. They incorporated a Poisson's effect, which was often neglected in 1D laminated beam analysis, in the formulation of the beam constitutive equation. Shi and Lam [5] presented the derivation of the variational consistent stiffness and mass matrices for the FE modeling of a composite beam. The two-noded higher-order composite beam element possessed a linear bending strain as opposed to the constant bending strain in the existing higher-order composite beam elements with the same number of nodal degrees of freedom (dof) [3,4,6]. A higher-order shear deformation theory and the conventional first-order theory were used by Maiti and Sinha [7] to develop a FE method to analyze accurately the free vibration behavior of laminated composites, using nine-noded rectangular isoparametric elements. Rao and Ganesan [9] examined the harmonic response of tapered composite beams using the FE analysis based on the higher-order shear deformation theory. Nabi and Ganesan [9] studied bi-axial bending, axial and torsional vibrations using the FE method and the first-order shear deformation theory. Hodges et al. [10] solved the equations of motion by a mixed FE method, and compared the FE results with an exact integration method, based on the transfer matrix approach. They showed that the free vibration characteristics of composite beams are sensitive to the assumptions used in determining the cross-sectional stiffnesses. Stemple and Lee [11] successfully employed their finite-element-based structural model with dynamic analysis and presented the vibrational characteristics of both solid and thin-walled cross-section as a function of their angular velocity. Also a two-noded, 10 dof per node, laminated composite thin-walled beam FE was developed by Wu and Sun [12] for vibration analysis based on modified assumptions of classical isotropic thin-walled beam theory. Gupta et al. [13] derived a two-noded, 8 dof per node, beam FE for laminated anisotropic thin-walled beams with open section. The displacements of the element reference axes were expressed in terms of 1D first-order Hermitian interpolation polynomials.

On the other hand, considerable research [14–24] for analytical solutions of the vibrational analysis of composite beams has been done. Cortínez and Piovan [14] obtained an analytical solution of the developed equation for the case of simply supported thin-walled beams with open or closed cross-section for free vibration problems in a unified fashion. also for calculating the circular frequencies of freely vibrating beams; Closed-form solutions were derived by Kollár [15] for the simply supported thin-walled open section composite beam including the effect of shear deformations and an approximate solution was also suggested. Matsunaga [16] derived a set of fundamental dynamic equations of a 1D higher-order theory for laminated composite beams through Hamilton's principle by using the method of power series expansion of displacement components. Song and Librescu [17] presented an analytical study devoted to the mathematical modeling of spinning anisotropic thin-walled beams. Special attention was paid to the influence played by anisotropy of constituent materials, boundary conditions and spinning speed on forward and backward precession frequencies and on instability speed. Also they [18] proposed an analytical model for dynamic analysis of anisotropic composite thin-walled closed beams. This model took into account the shear flexibility due to bending displacements in addition to primary and secondary warping effects. Song and Waas [19] studied the free vibration solution of stepped laminated composite beams of rectangular cross-section using a simple higher-order theory which assumes a cubic distribution for the displacement field through the thickness. They used a method of separation of variables to governing equations and obtained 12 homogenous linear algebraic

equations by applying appropriate boundary conditions. then; They obtained the solutions of homogeneous equation using a numerical solver. Teboub and Hajela [20] used a first-order shear deformation theory to analyze the free vibrations of generally layered composite beams. The equations of motion were integrated with the aid of a symbolic manipulation program. Various results have been included to show the effects of the beam geometry, boundary conditions, Poisson's effect, material anisotropy, and coupling of stiffnesses, on the natural frequencies of composite beams. The study by Farghaly and Gadelrab [21] who used exact analytical solutions was concerned with an additional expected gain in natural frequencies for a one-span beam with a stepwise variable cross-section made of unidirectional fiber composite materials of different fiber volume fraction. A theoretical study of the free vibration characteristics of thin-walled composite blades has been presented by Rand [22]. The exact solutions for the natural frequencies of symmetrically laminated composite beams have been predicted by Chandrashekhara et al. [23] using the first-order shear deformation theory. The numerical analysis was based on reducing a detailed structural formulation, which included an out-of-plane warping deformation to a beam-type formulation. Vinson and Sierakowski [24] obtained the exact solution of a simply supported composite beam based on the classical theory.

As an alternative approach to calculate the natural frequency of composite beam, the transfer matrix method has been used in Refs. [25–27]. Yildirim et al. [25] studied in-plane and out-of-plane free vibration problems of symmetric cross-ply laminated composite beams using the transfer matrix method. Thereafter, as a continuation of Yildirim et al. [25], Yildirim and Kiral [26] performed the out-of-plane free vibration analysis of symmetric cross-ply laminated composite beams. The relative difference between the 1st six non-dimensional frequencies obtained by the Bernoulli–Euler and Timoshenko beam theories was presented for different length to thickness ratios, thickness to width ratios and different type of boundary conditions. Khdeir and Reddy [27] employed the transfer matrix method in the free vibration analysis of cross-ply laminated beams based on the higher-order shear deformation theory.

Another effective method solving the dynamic problem of composite beams was to develop the exact dynamic stiffness matrix based on the solution of the simultaneous ordinary differential equations. Banerjee and Williams [28,29] have developed the dynamic stiffness matrices of a composite beam [28] and a composite Timoshenko beam [29] in order to investigate their free vibration characteristics. The associated theories accounted for the effect of the material coupling between the bending and torsional modes of deformation which is usually present in composite beams, such as aircraft wings. And an explicit analytical expression for each of the elements of the dynamic stiffness was derived by rigorous use of the symbolic computing package. Thereafter, Banerjee [30] extended the earlier theories of Banerjee and Williams [28,29] by including the effect of an axial force. Also Banerjee [31] derived analytical expressions for the frequency equation and mode shapes of a bending–torsion materially coupled composite Timoshenko beam with cantilever end condition in explicit form using the symbolic computing package. Abramovich [32] presented exact solutions for symmetrically laminated beams with 10 different boundary conditions using the exact element method. This exact element method uses the exact shape functions of the beam that are represented by converging infinite series. Using these shape functions, the solution can be obtained with any desired accuracy yielding the exact one. Abramovich and Livshits [33] extended the approach of Abramovich [32] to include non-symmetric lay-ups. Also Abramovich et al. [34] applied the exact element method to calculate the natural frequencies and the influence of the axial load on the natural frequencies and mode shapes of non-symmetric laminated composite beams. Dynamic stiffness analysis of symmetric and non-symmetric cross-ply laminated beams has been presented by using a first-order shear deformation theory by Eisenberger et al. [35]. However, the above-mentioned works [28–35] considered only the dynamic stiffness of composite beam with rectangular cross-section.

Even though a significant amount of research has been conducted on development of improved composite beam elements, to the best of authors' knowledge, there was no study reported on the exact solutions for the free vibration analysis of thin-walled composite beam with arbitrary lamination in the literature. The dynamic behavior of thin-walled composite beam with arbitrary lamination is very complex due to the coupling effect of extensional, bending, and torsional deformations and many researchers thought that it is too complex to solve the vibrational problem exactly for the spatially coupled thin-walled composite beam due to an aforementioned reason.

The aim of this study is to present the exact dynamic stiffness matrix that can be used in analyzing the free vibrational behavior of thin-walled I-beam made from fiber-reinforced laminates with symmetric and arbitrary laminations. A significant point of departure of the present approach from other methods is in the solution of spatially coupled equations of motion that arise in the solutions scheme. Rather than using a discrete integration scheme or a method based on energy principles which may perform poorly for stiff systems, the present approach advocates the use of direct evaluation schemes using symbolic manipulation. The important points presented are summarized as follows:

1. A general theory is developed for the free vibration analysis of thin-walled composite beam with arbitrary lamination.
2. The numerical method using a generalized linear eigenproblem having complex eigenvalues to evaluate exactly the dynamic stiffness matrix of thin-walled composite beam is presented.
3. In addition, the FE procedure using the Hermitian beam elements including the restrained warping effect is presented.
4. To verify the validity and the accuracy of this study, the natural frequencies of composite I-beam with various boundary conditions are evaluated and compared with analytical solutions by other researchers, the results from available references and the FE analysis using the thin-walled Hermitian beam elements. Particularly, the mode change phenomenon, the effects of increase of the modulus and the bending–twisting coupling stiffness for beams with various boundary conditions are investigated.

2. Vibration theory of thin-walled composite beam with arbitrary lamination

In this study, for the spatially coupled vibration analysis of a thin-walled composite beam with arbitrary lamination, the classical Vlasov's assumptions are adopted. Fig. 1 shows three sets of coordinate systems which are mutually interrelated; an orthogonal Cartesian coordinate global system (x_1, x_2, x_3) for the beam, an orthogonal local coordinate system (n, s, x_1) for the plate segment of the beam, where the n axis is the normal to the mid-surface of any plate segment and the s axis is tangential to the mid-surface along the contour line of the beam cross section; and a contour coordinate system S, where S is measured along the contour line of the cross section from a chosen origin O. The point P denotes the pole axis and is placed at an arbitrary point y_p and z_p. Figs. 2a and b show the nodal displacements and force vectors, respectively,

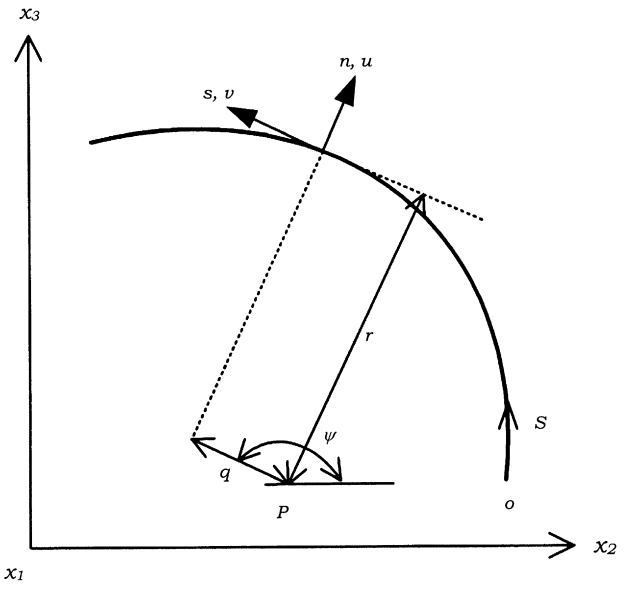

Fig. 1. Pictorial definitions of coordinates in thin-walled section.

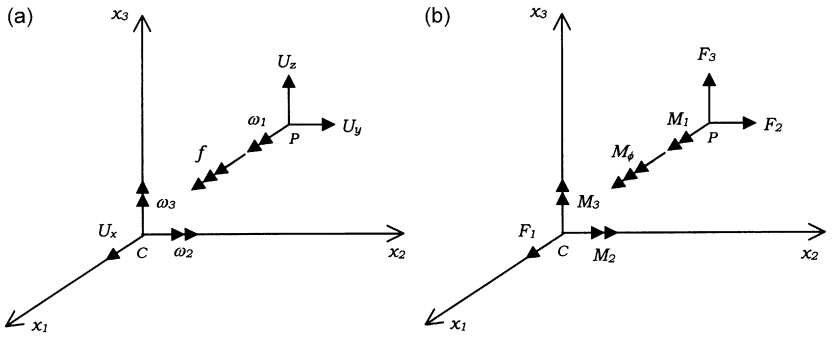

Fig. 2. Displacement parameters and stress resultants.

Under consideration where U_x, U_y, and U_z and $\omega_1(=\theta)$, $\omega_2(=-U_z')$, and $\omega_3(=-U_y')$ are rigid body translations and rotations with respect to x_1-, x_2-, and x_3-axis, respectively, and $f(-\theta')$ is the warping parameter. From the study by Gjelsvik [36], displacement components u, v, and w of arbitrary points in the contour coordinate system can be expressed as follows:

$$u(s,x_1) = U_y(x_1)\sin\psi(s) - U_z(x_1)\cos\psi(s) - \theta(x_1)q(s) \tag{1a}$$

$$v(s,x_1) = U_y(x_1)\cos\psi(s) + U_z(x_1)\sin\psi(s) + \theta(x_1)r(s) \tag{1b}$$

$$w(s,x_1) = U_x(x_1) - U_y'(x_1)x_2 - U_z'(x_1)x_3 - \theta'(x_1)\phi \tag{1c}$$

where the prime indicates the differentiation with respect to x_1 and ϕ is the normalized warping function. The constitutive relations by Jones [37] for an arbitrary laminate are

$$\begin{Bmatrix} N_x \\ N_s \\ N_{xs} \\ M_x \\ M_s \\ M_{xs} \end{Bmatrix} = \begin{bmatrix} A_{11} & A_{12} & A_{16} & B_{11} & B_{12} & B_{16} \\ A_{12} & A_{22} & A_{26} & B_{12} & B_{22} & B_{26} \\ A_{16} & A_{26} & A_{66} & B_{16} & B_{26} & B_{66} \\ B_{11} & B_{12} & B_{16} & D_{11} & D_{12} & D_{16} \\ B_{12} & B_{22} & B_{26} & D_{12} & D_{22} & D_{26} \\ B_{16} & B_{26} & B_{66} & D_{16} & D_{26} & D_{66} \end{bmatrix} \begin{Bmatrix} \varepsilon_x \\ \varepsilon_s \\ \gamma_{xs} \\ \kappa_x \\ \kappa_s \\ \kappa_{xs} \end{Bmatrix} \tag{2}$$

where

$$A_{ij} = \sum_{k=1}^{N} \bar{Q}_{ij}^k (t_k - t_{k-1}) = t a_{ij} \tag{3a}$$

$$B_{ij} = \frac{1}{2}\sum_{k=1}^{N} \bar{Q}_{ij}^k (t_k^2 - t_{k-1}^2) = t^2 b_{ij} \tag{3b}$$

$$D_{ij} = \frac{1}{3}\sum_{k=1}^{N} \bar{Q}_{ij}^k (t_k^3 - t_{k-1}^3) = t^3 d_{ij} \tag{3c}$$

In the above equations, A_{ij}, B_{ij}, and D_{ij} are the extensional, bending–extension coupling, and bending stiffnesses, respectively. Also $\bar{Q}_{ij}$ denotes the lamina stiffness coefficient; ε_x, ε_s, and γ_{xs} are the membrane strains of lamina; k_x, k_s, and k_{xs} are the axial, tangential, and twist curvatures, respectively, of middle surface.

Based on the principle of virtual work [36], beam stress resultants are equivalent to distributions of plate stress resultants acting on a cross section of a beam and these relationships between beam stress resultants and plate ones are presented in Appendix A.

Recently, based on these transformation relationships and constitutive relations between the beam stress resultants and the displacements, the Shin et al. [38] derived the elastic strain energy of thin-walled composite

beam with arbitrary lamination during a displacement of the cross-section as follows:

$$\Pi_E = \frac{1}{2}\int_o^l \Big[A U'^2_x + I_3 U''^2_y + I_2 U''^2_z + 2I_{23} U''_y U''_z + I_\phi \theta''^2 + 2I_{\phi 3} U''_y \theta'' + 2I_{\phi 2} U''_z \theta'' + JG\theta'^2 - 2S_2 U'_x U''_z - 2S_3 U'_x U''_y - 2S_w U'_x \theta'' + 2S_\phi U'_x \theta' - 2H_s U''_y \theta' + 2H_c U''_z \theta' + 2H_q \theta' \theta'' \Big] \mathrm{d}x_1 \tag{4}$$

where l denotes the length of beam and the detailed expressions of sectional quantities in Eq. (4) are presented in Appendix B.

Also, the kinetic energy Π_M of the beam considering the rotary inertia effect is given by

$$\Pi_M = \frac{1}{2}\int_V \rho(\dot{u}^2 + \dot{v}^2 + \dot{w}^2)\,\mathrm{d}V \tag{5}$$

where ρ is the density and substitution of displacement components into Eq. (5) leads to

$$\Pi_M = \frac{1}{2}\rho\omega^2 \int_o^l \Big[A^*(U_x^2 + U_y^2 + U_z^2) + I_2^* U'^2_z + I_3^* U'^2_y + I_o^* \theta^2 + I_\phi^* \theta'^2 + 2I_{23}^* U'_y U'_z + 2I_{\phi 2}^* U'_z \theta' + 2I_{\phi 3}^* U'_y \theta' + 2A^*(y - y_p) U_z \theta - 2A^*(z - z_p) U_y \theta \Big] \mathrm{d}x_1 \tag{6}$$

where ω is the frequency of harmonic vibration; A^*, I_2^*, I_3^*, I_o^*, I_{23}^* and I_ϕ^* are the cross-sectional area, the 2nd moment of inertia about x_2 and x_3 axes, the polar moment of inertia, the product moment of inertia and the warping moment of inertia, respectively. $I_{\phi 2}^*$ and $I_{\phi 3}^*$ are the product moments of inertia due to the normalized warping. These section properties are defined as follows:

$$A^* = \int_{A^*} \mathrm{d}A^* \tag{7a}$$

$$I_2^* = \int_{A^*} x_3^2\,\mathrm{d}A^* \tag{7b}$$

$$I_3^* = \int_{A^*} x_2^2\,\mathrm{d}A^* \tag{7c}$$

$$I_o^* = \int_{A^*} (q^2 + r^2)\,\mathrm{d}A^* \tag{7d}$$

$$I_{23}^* = \int_{A^*} x_2 x_3\,\mathrm{d}A^* \tag{7e}$$

$$I_\phi^* = \int_{A^*} \phi^2\,\mathrm{d}A^* \tag{7f}$$

$$I_{\phi 2}^* = \int_{A^*} \phi x_3\,\mathrm{d}A^* \tag{7g}$$

$$I_{\phi 3}^* = \int_{A^*} \phi x_2\,\mathrm{d}A^* \tag{7h}$$

In Eq. (6), the following geometric relations are used from Fig. 1:

$$y - y_P = q\cos\psi + r\sin\psi \tag{8a}$$

$$z - z_P = q\sin\psi - r\cos\psi \tag{8b}$$

Then, we consider the following total potential energy:

$$\Pi_T = \Pi_E - \Pi_M - \Pi_{\text{ext}} \tag{9}$$

where Π_{ext} is the external work corresponding to the element nodal forces.

Finally, by variation of the total potential energy with respect to displacement components U_x, U_y, U_z, and θ, the equations of motion for the spatially coupled free vibration analysis of thin-walled composite beam with arbitrary lamination are derived as follows:

$$AU_x'' - S_3U_y''' - S_2U_z''' + S_\phi\theta'' - S_w\theta''' + \rho\omega^2A^*U_x = 0 \tag{10}$$

$$\begin{aligned}&- S_3U_x''' + I_3U_y'''' + I_{23}U_z'''' - H_s\theta''' + I_{\phi3}\theta''''\\&- \rho\omega^2\left[A^*U_y - I_3^*U_y'' - I_{23}^*U_z'' - A^*(z-z_P)\theta - I_{\phi3}^*\theta''\right] = 0\end{aligned} \tag{11}$$

$$\begin{aligned}&- S_2U_x''' + I_{23}U_y'''' + I_2U_z'''' + H_c\theta''' + I_{\phi2}\theta''''\\&- \rho\omega^2\left[-I_{23}^*U_y'' + A^*U_z - I_2^*U_z'' + A^*(y-y_P)\theta - I_{\phi2}^*\theta''\right] = 0\end{aligned} \tag{12}$$

$$\begin{aligned}&- S_\phi U_x'' - S_wU_x''' + H_sU_y''' + I_{\phi3}U_y'''' - H_cU_z''' + I_{\phi2}U_z'''' - JG\theta'' + I_\phi\theta''''\\&- \rho\omega^2\left[-A^*(z-z_P)U_y - I_{\phi3}^*U_y'' + A^*(y-y_P)U_z - I_{\phi2}^*U_z'' + I_o^*\theta - I_\phi^*\theta''\right] = 0\end{aligned} \tag{13}$$

From Eq. (10), we can obtain the following equation:

$$U_x''' = \frac{S_3}{A}U_y'''' + \frac{S_2}{A}U_z'''' - \frac{S_\phi}{A}\theta''' + \frac{S_w}{A}\theta'''' - \rho\omega^2\frac{A^*}{A}U_x' \tag{14}$$

Substituting Eq. (14) into Eqs. (11)–(13), Eqs. (11)–(13) can be rewritten as

$$\begin{aligned}&\tilde{I}_3U_y'''' + \tilde{I}_{23}U_z'''' - \tilde{H}_s\theta''' + \tilde{I}_{\phi3}\theta''''\\&+ \rho\omega^2\left[\frac{A^*}{A}S_3U_x' - A^*U_y + I_3^*U_y'' + I_{23}^*U_z'' + A^*(z-z_P)\theta + I_{\phi3}^*\theta''\right] = 0\end{aligned} \tag{15}$$

$$\begin{aligned}&\tilde{I}_{23}U_y'''' + \tilde{I}_2U_z'''' + \tilde{H}_c\theta''' + \tilde{I}_{\phi2}\theta''''\\&+ \rho\omega^2\left[\frac{A^*}{A}S_2U_x' - A^*U_z + I_{23}^*U_y'' + I_2^*U_z'' - A^*(y-y_P)\theta + I_{\phi2}^*\theta''\right] = 0\end{aligned} \tag{16}$$

$$\begin{aligned}&- S_\phi U_x'' + H_sU_y''' + \tilde{I}_{\phi3}U_y'''' - H_cU_z''' + \tilde{I}_{\phi2}U_z'''' - JG\theta'' + \frac{S_\phi S_w}{A}\theta''' + \tilde{I}_\phi\theta''''\\&+ \rho\omega^2\left[\frac{A^*}{A}S_wU_x' + A^*(z-z_P)U_y + I_{\phi3}^*U_y'' - A^*(y-y_P)U_z + I_{\phi2}^*U_z'' - I_o^*\theta + I_\phi^*\theta''\right] = 0\end{aligned} \tag{17}$$

where

$$\begin{gathered}\tilde{I}_2 = I_2 - \frac{S_2^2}{A},\quad \tilde{I}_3 = I_3 - \frac{S_3^2}{A},\quad \tilde{I}_{23} = I_{23} - \frac{S_2S_3}{A},\quad \tilde{I}_\phi = I_\phi - \frac{S_w^2}{A},\quad \tilde{I}_{\phi2} = I_{\phi2} - \frac{S_2S_w}{A},\\ \tilde{I}_{\phi3} = I_{\phi3} - \frac{S_3S_w}{A},\quad \tilde{H}_s = H_s - \frac{S_3S_\phi}{A},\quad \tilde{H}_c = H_c + \frac{S_2S_\phi}{A}\end{gathered} \tag{18a–h}$$

and geometric and natural boundary conditions are as follows:

$$\delta U_x(o) = \delta U_x^p \text{ or } F_1(o) = -F_1^p,\quad \delta U_x(l) = \delta U_x^q \text{ or } F_1(l) = F_1^q \tag{19a,b}$$

$$\delta U_y(o) = \delta U_y^p \text{ or } F_2(o) = -F_2^p,\quad \delta U_y(l) = \delta U_y^q \text{ or } F_2(l) = F_2^q \tag{19c,d}$$

$$\delta U_z(o) = \delta U_z^p \text{ or } F_3(o) = -F_3^p,\quad \delta U_z(l) = \delta U_z^q \text{ or } F_3(l) = F_3^q \tag{19e,f}$$

$$\delta\theta(o) = \delta\omega_1^p \text{ or } M_1(o) = -M_1^p, \quad \delta\theta(l) = \delta\omega_1^q \text{ or } M_1(l) = M_1^q \tag{19g,h}$$

$$-\delta U_z'(o) = \delta\omega_2^p \text{ or } M_2(o) = -M_2^p, \quad -\delta U_z'(l) = \delta\omega_2^q \text{ or } M_2(l) = M_2^q \tag{19i,j}$$

$$\delta U_y'(o) = \delta\omega_3^p \text{ or } M_3(o) = -M_3^p, \quad \delta U_y'(l) = \delta\omega_3^q \text{ or } M_3(l) = M_3^q \tag{19k,l}$$

$$-\delta\theta(o) = \delta f^p \text{ or } M_\phi(o) = -M_\phi^p, \quad -\delta\theta(l) = \delta f^q \text{ or } M_\phi(l) = M_\phi^q \tag{19m,n}$$

and force–displacement relationships are as follows:

$$F_1 = AU_x' - S_3U_y'' - S_2U_z'' + S_\phi\theta' - S_w\theta'' \tag{20a}$$

$$F_2 = -\tilde{I}_3U_y''' - \tilde{I}_{23}U_z''' + \tilde{H}_s\theta'' - \tilde{I}_{\phi 3}\theta''' - \rho\omega^2\left(\frac{A^*}{A}S_3U_x + I_3^*U_y' + I_{23}^*U_z' + I_{\phi 3}^*\theta'\right) \tag{20b}$$

$$F_3 = -\tilde{I}_{23}U_y''' - \tilde{I}_2U_z''' - \tilde{H}_c\theta'' - \tilde{I}_{\phi 2}\theta''' - \rho\omega^2\left(\frac{A^*}{A}S_2U_x + I_{23}^*U_y' + I_2^*U_z' + I_{\phi 2}^*\theta'\right) \tag{20c}$$

$$M_1 = S_\phi U_x' - H_sU_y'' - \tilde{I}_{\phi 3}U_y''' + H_cU_z'' - \tilde{I}_{\phi 2}U_z''' + JG\theta' - \frac{S_\phi S_w}{A}\theta'' - \tilde{I}_\phi\theta''' - \rho\omega^2\left(\frac{A^*}{A}S_wU_x + I_{\phi 3}^*U_y' - I_{\phi 2}^*U_z' + I_\phi^*\theta'\right) \tag{20d}$$

$$M_2 = S_2U_x' - I_{23}U_y'' - I_2U_z'' - H_c\theta' - I_{\phi 2}\theta'' \tag{20e}$$

$$M_3 = -S_3U_x' + I_3U_y'' + I_{23}U_z'' - H_s\theta' + I_{\phi 3}\theta'' \tag{20f}$$

$$M_\phi = S_wU_x' - I_{\phi 3}U_y'' - I_{\phi 2}U_z'' - H_q\theta' - I_\phi\theta'' \tag{20g}$$

3. Exact dynamic stiffness matrix

3.1. Exact evaluation of displacement function

The exact displacement function for the vibration analysis of thin-walled composite beam with symmetric and arbitrary laminations is evaluated. Eq. (10) and Eqs. (15)–(17) are the simultaneous ordinary differential equations of the fourth order. To transform these equations into the simultaneous differential equations of the first order, a displacement state vector consisting of 14 displacement parameters is defined by

$$\mathbf{d} = \left\langle U_x, U_x', U_y, U_y', U_y'', U_y''', U_z, U_z', U_z'', U_z''', \theta, \theta', \theta'', \theta''' \right\rangle^{\mathrm{T}} = \langle d_1, d_2, d_3, d_4, d_5, d_6, d_7, d_8, d_9, d_{10}, d_{11}, d_{12}, d_{13}, d_{14} \rangle^{\mathrm{T}} \tag{21}$$

Based on Eq. (21), Eqs. (10) and (15)–(17) are transformed into the following simultaneous ordinary differential equations of the first order with constant coefficients

$$d_1' = d_2 \tag{22a}$$

$$Ad_2' = -\rho\omega^2A^*d_1 + S_3d_6 + S_2d_{10} - S_\phi d_{13} + S_wd_{14} \tag{22b}$$

$$d_3' = d_4 \tag{22c}$$

$$d_4' = d_5 \tag{22d}$$

$$d'_5 = d_6 \tag{22e}$$

$$\begin{aligned}\tilde{I}_3 d'_6 + \tilde{I}_{23} d'_{10} + \tilde{I}_{\phi 3} d'_{14} = & -\rho\omega^2 \frac{A^*}{A} S_3 d_2 + \rho\omega^2 A^* d_3 - \rho\omega^2 I^*_3 d_5 - \rho\omega^2 I^*_{23} d_9 \\ & - \rho\omega^2 A^*(z - z_P) d_{11} - \rho\omega^2 I^*_{\phi 3} d_{13} + \tilde{H}_s d_{14}\end{aligned} \tag{22f}$$

$$d'_7 = d_8 \tag{22g}$$

$$d'_8 = d_9 \tag{22h}$$

$$d'_9 = d_{10} \tag{22i}$$

$$\begin{aligned}\tilde{I}_{23} d'_6 + \tilde{I}_2 d'_{10} + \tilde{I}_{\phi 2} d'_{14} = & -\rho\omega^2 \frac{A^*}{A} S_2 d_2 - \rho\omega^2 I^*_{23} d_5 + \rho\omega^2 A^* d_7 - \rho\omega^2 I^*_2 d_9 \\ & + \rho\omega^2 A^*(y - y_P) d_{11} - \rho\omega^2 I^*_{\phi 2} d_{13} - \tilde{H}_c d_{14}\end{aligned} \tag{22j}$$

$$d'_{11} = d_{12} \tag{22k}$$

$$d'_{12} = d_{13} \tag{22l}$$

$$d'_{13} = d_{14} \tag{22m}$$

$$\begin{aligned}-S_\phi d'_2 + \tilde{I}_{\phi 3} d'_6 + \tilde{I}_{\phi 2} d'_{10} + \tilde{I}_\phi d'_{14} = & -\rho\omega^2 \frac{A^*}{A} S_w d_2 - \rho\omega^2 A^*(z - z_P) d_3 - \rho\omega^2 I^*_{\phi 3} d_5 \\ & - H_s d_6 + \rho\omega^2 A^*(y - y_P) d_7 - \rho\omega^2 I^*_{\phi 2} d_9 + H_c d_{10} + \rho\omega^2 I^*_o d_{11} \\ & + (JG - \rho\omega^2 I^*_\phi) d_{13} - \frac{S_\phi S_w}{A} d_{14}\end{aligned} \tag{22n}$$

which can be compactly expressed as

$$\mathbf{A}\mathbf{d}' = \mathbf{B}\mathbf{d} \tag{23}$$

where the components of matrices **A** and **B** are given in Appendix C.

In order to find the homogeneous solution of the simultaneous differential Eq. (23), the following eigenvalue problem with non-symmetric matrix is taken into account:

$$\lambda \mathbf{A}\mathbf{Z} = \mathbf{B}\mathbf{Z} \tag{24}$$

In practice, the general eigenvalue problem of Eq. (24) has the complex eigenvalue and the associated eigenvector because the matrix **A** is symmetric but **B** is non-symmetric. An IMSL subroutine DGVCRG (IMSL Library [39]) is adopted so that eigensolutions of 14 pairs are calculated as follows:

$$(\lambda_i, \mathbf{Z}_i), \quad i = 1, 2, \ldots, 14 \tag{25}$$

where

$$\mathbf{Z}_i = \langle z_{1,i}, z_{2,i}, z_{3,i}, z_{4,i}, z_{5,i}, z_{6,i}, z_{7,i}, z_{8,i}, z_{9,i}, z_{10,i}, z_{11,i}, z_{12,i}, z_{13,i}, z_{14,i} \rangle^{\mathrm{T}} \tag{26}$$

It is possible that the general solution of Eq. (23) is represented as the linear combination of eigenvectors with complex exponential functions

$$\mathbf{d}(\mathbf{x}) = \sum_{i=1}^{14} a_i \mathbf{Z}_i \, \mathrm{e}^{\lambda_i x} = \mathbf{X}(\mathbf{x})\mathbf{a} \tag{27}$$

where

$$\begin{aligned}\mathbf{X}(\mathbf{x}) = \big[& \mathbf{Z}_1 \, \mathrm{e}^{\lambda_1 x}, \ \mathbf{Z}_2 \, \mathrm{e}^{\lambda_2 x}, \ \mathbf{Z}_3 \, \mathrm{e}^{\lambda_3 x}, \ \mathbf{Z}_4 \, \mathrm{e}^{\lambda_4 x}, \ \mathbf{Z}_5 \, \mathrm{e}^{\lambda_5 x}, \ \mathbf{Z}_6 \, \mathrm{e}^{\lambda_6 x}, \ \mathbf{Z}_7 \, \mathrm{e}^{\lambda_7 x}, \\ & \mathbf{Z}_8 \, \mathrm{e}^{\lambda_8 x}, \ \mathbf{Z}_9 \, \mathrm{e}^{\lambda_9 x}, \ \mathbf{Z}_{10} \, \mathrm{e}^{\lambda_{10} x}, \ \mathbf{Z}_{11} \, \mathrm{e}^{\lambda_{11} x}, \ \mathbf{Z}_{12} \, \mathrm{e}^{\lambda_{12} x}, \ \mathbf{Z}_{13} \, \mathrm{e}^{\lambda_{13} x}, \ \mathbf{Z}_{14} \, \mathrm{e}^{\lambda_{14} x} \big]\end{aligned} \tag{28a}$$

$$\mathbf{a} = \langle a_1, a_2, a_3, a_4, a_5, a_6, a_7, a_8, a_9, a_{10}, a_{11}, a_{12}, a_{13}, a_{14} \rangle^{\mathrm{T}} \tag{28b}$$

In Eq. (28), $\mathbf{X}(\mathbf{x})$ and $\mathbf{a}$ are the 14×14 matrix function made up of 14 eigensolutions and the integration constants, respectively.

Next the complex coefficients $\mathbf{a}$ is represented with respect to 14 nodal displacement components. For this, the nodal displacement vector at p and q which mean the two ends of the member ($x = 0$, l) is defined by

$$\mathbf{U}_e = \langle \mathbf{U}^p, \mathbf{U}^q \rangle^{\mathrm{T}} \tag{29a}$$

$$\mathbf{U}^\chi = \langle U_x^\chi, U_y^\chi, U_z^\chi, \omega_1^\chi, \omega_2^\chi, \omega_3^\chi, f^\chi \rangle^{\mathrm{T}}, \quad \chi = p, q \tag{29b}$$

where

$$\mathbf{U}^p = \langle U_x(o), U_y(o), U_z(o), \theta(o), -U_z'(o), U_y'(o), -\theta'(o) \rangle^{\mathrm{T}} \tag{30a}$$

$$\mathbf{U}^q = \langle U_x(l), U_y(l), U_z(l), \theta(l), -U_z'(l), U_y'(l), -\theta'(l) \rangle^{\mathrm{T}} \tag{30b}$$

By substituting coordinates of the member end ($x = 0$, l) into Eq. (27) and accounting for Eq. (29), nodal displacement vector $\mathbf{U}_e$ can be obtained as follows:

$$\mathbf{U}_e = \mathbf{E}\mathbf{a} \tag{31}$$

where $\mathbf{E}$ is evaluated from $\mathbf{X}(\mathbf{x})$ and presented as

$$\mathbf{E} = \begin{bmatrix}
z_{1,1} & z_{1,2} & z_{1,3} & z_{1,4} & z_{1,5} & z_{1,6} & z_{1,7} & z_{1,8} & z_{1,9} & z_{1,10} & z_{1,11} & z_{1,12} & z_{1,13} & z_{1,14} \\
z_{3,1} & z_{3,2} & z_{3,3} & z_{3,4} & z_{3,5} & z_{3,6} & z_{3,7} & z_{3,8} & z_{3,9} & z_{3,10} & z_{3,11} & z_{3,12} & z_{3,13} & z_{3,14} \\
z_{7,1} & z_{7,2} & z_{7,3} & z_{7,4} & z_{7,5} & z_{7,6} & z_{7,7} & z_{7,8} & z_{7,9} & z_{7,10} & z_{7,11} & z_{7,12} & z_{7,13} & z_{7,14} \\
z_{11,1} & z_{11,2} & z_{11,3} & z_{11,4} & z_{11,5} & z_{11,6} & z_{11,7} & z_{11,8} & z_{11,9} & z_{11,10} & z_{11,11} & z_{11,12} & z_{11,13} & z_{11,14} \\
-z_{8,1} & -z_{8,2} & -z_{8,3} & -z_{8,4} & -z_{8,5} & -z_{8,6} & -z_{8,7} & -z_{8,8} & -z_{8,9} & -z_{8,10} & -z_{8,11} & -z_{8,12} & -z_{8,13} & -z_{8,14} \\
z_{4,1} & z_{4,2} & z_{4,3} & z_{4,4} & z_{4,5} & z_{4,6} & z_{4,7} & z_{4,8} & z_{4,9} & z_{4,10} & z_{4,11} & z_{4,12} & z_{4,13} & z_{4,14} \\
-z_{12,1} & -z_{12,2} & -z_{12,3} & -z_{12,4} & -z_{12,5} & -z_{12,6} & -z_{12,7} & -z_{12,8} & -z_{12,9} & -z_{12,10} & -z_{12,11} & -z_{12,12} & -z_{12,13} & -z_{12,14} \\
y_{1,1} & y_{1,2} & y_{1,3} & y_{1,4} & y_{1,5} & y_{1,6} & y_{1,7} & y_{1,8} & y_{1,9} & y_{1,10} & y_{1,11} & y_{1,12} & y_{1,13} & y_{1,14} \\
y_{3,1} & y_{3,2} & y_{3,3} & y_{3,4} & y_{3,5} & y_{3,6} & y_{3,7} & y_{3,8} & y_{3,9} & y_{3,10} & y_{3,11} & y_{3,12} & y_{3,13} & y_{3,14} \\
y_{7,1} & y_{7,2} & y_{7,3} & y_{7,4} & y_{7,5} & y_{7,6} & y_{7,7} & y_{7,8} & y_{7,9} & y_{7,10} & y_{7,11} & y_{7,12} & y_{7,13} & y_{7,14} \\
y_{11,1} & y_{11,2} & y_{11,3} & y_{11,4} & y_{11,5} & y_{11,6} & y_{11,7} & y_{11,8} & y_{11,9} & y_{11,10} & y_{11,11} & y_{11,12} & y_{11,13} & y_{11,14} \\
-y_{8,1} & -y_{8,2} & -y_{8,3} & -y_{8,4} & -y_{8,5} & -y_{8,6} & -y_{8,7} & -y_{8,8} & -y_{8,9} & -y_{8,10} & -y_{8,11} & -y_{8,12} & -y_{8,13} & -y_{8,14} \\
y_{4,1} & y_{4,2} & y_{4,3} & y_{4,4} & y_{4,5} & y_{4,6} & y_{4,7} & y_{4,8} & y_{4,9} & y_{4,10} & y_{4,11} & y_{4,12} & y_{4,13} & y_{4,14} \\
-y_{12,1} & -y_{12,2} & -y_{12,3} & -y_{12,4} & -y_{12,5} & -y_{12,6} & -y_{12,7} & -y_{12,8} & -y_{12,9} & -y_{12,10} & -y_{12,11} & -y_{12,12} & -y_{12,13} & -y_{12,14}
\end{bmatrix} \tag{32}$$

where

$$y_{i,j} = z_{i,j}\, \mathrm{e}^{\lambda_j l}, \quad i = 1, 3, 7, 11, 8, 4, 12, \;\; j = 1\text{–}14 \tag{33}$$

Elimination of the complex coefficients $\mathbf{a}$ from Eq. (27) using Eq. (31) yields the displacement state vector consisting of 14 displacement components

$$\mathbf{d}(\mathbf{x}) = \mathbf{X}(\mathbf{x})\mathbf{E}^{-1}\mathbf{U}_e \tag{34}$$

where $\mathbf{X}(\mathbf{x})\mathbf{E}^{-1}$ denotes the exact interpolation matrix. In Eq. (34), the inverse of $\mathbf{E}$ is calculated using an IMSL subroutine DLINCG (IMSL Library [39]).

3.2. Calculation of dynamic stiffness matrix

Now, we consider the nodal force vector at two ends p and q defined by

$$\mathbf{F}_e = \langle \mathbf{F}^p, \mathbf{F}^q \rangle^{\mathrm{T}} \tag{35}$$

where

$$\mathbf{F}^{\chi} = \langle F_1^{\chi}, F_2^{\chi}, F_3^{\chi}, M_1^{\chi}, M_2^{\chi}, M_3^{\chi}, M_{\phi}^{\chi}\rangle^{\mathrm{T}}, \quad \chi = p, q \tag{36}$$

Using Eqs. (21), the force–displacement relationships in Eqs. (20a–g) of thin-walled composite beam can be compactly rewritten as follows:

$$\mathbf{f}(\mathbf{x}) = \mathbf{S}\mathbf{d}(\mathbf{x}) \tag{37}$$

where $\mathbf{f} = \langle F_1, F_2, F_3, M_1, M_2, M_3, M_{\phi}\rangle^{\mathrm{T}}$ and each element of 7×14 matrix $\mathbf{S}$ is presented in Appendix C.

Then substituting Eq. (34) into Eq. (37) leads to

$$\mathbf{f}(\mathbf{x}) = \mathbf{S}\mathbf{X}(\mathbf{x})\mathbf{E}^{-1}\mathbf{U}_e \tag{38}$$

And nodal forces at ends of element are evaluated as

$$\mathbf{F}^{p} = -\mathbf{f}(0) = -\mathbf{S}\mathbf{X}(0)\mathbf{E}^{-1}\mathbf{U}_e \tag{39a}$$

$$\mathbf{F}^{q} = \mathbf{f}(l) = \mathbf{S}\mathbf{X}(l)\mathbf{E}^{-1}\mathbf{U}_e \tag{39b}$$

Consequently the exact dynamic stiffness matrix $\mathbf{K}(\boldsymbol{\omega})$ of a thin-walled composite beam with arbitrary lamination is calculated as follows:

$$\mathbf{F}_e = \mathbf{K}(\boldsymbol{\omega})\mathbf{U}_e \tag{40}$$

where

$$\mathbf{K}(\boldsymbol{\omega}) = \begin{bmatrix} -\mathbf{S}\mathbf{X}(0)\mathbf{E}^{-1} \\ \mathbf{S}\mathbf{X}(l)\mathbf{E}^{-1} \end{bmatrix} \tag{41}$$

The natural frequencies of vibration for the member are the values of ω that cause the dynamic stiffness matrix for the element to become singular as in Eq. (42). Here the incremental search method is applied to find these values up to the desired accuracy

$$\det\left|\mathbf{K}(\boldsymbol{\omega})\right| = 0 \tag{42}$$

It should be noted that the dynamic stiffness matrix in Eq. (42) is formed by frequency-dependent shape functions which are exact solutions of the governing differential equations. Therefore, it eliminates discretization errors and is capable of predicting an infinite number of natural frequencies by means of a finite number of coordinates.

4. Finite element formulation

For the purpose of comparing the natural frequencies evaluated from the present dynamic stiffness matrix with those from the numerical method, the FE model for thin-walled composite beam including the effects of the arbitrary lamination and the restrained warping is presented. To accurately express the element deformation, pertinent shape functions are necessary. Assuming that axial displacement is linear, the element displacement parameters can be interpolated as follows:

$$U_x = \eta U_x^{\xi} + (1-\eta)U_x^{\zeta} \tag{43a}$$

$$U_y = h_1 U_y^{\xi} + h_2\omega_3^{\xi} + h_3 U_y^{\zeta} + h_4\omega_3^{\zeta} \tag{43b}$$

$$U_z = h_1 U_z^{\xi} - h_2\omega_2^{\xi} + h_3 U_z^{\zeta} - h_4\omega_2^{\zeta} \tag{43c}$$

$$\theta = h_1\omega_1^{\xi} - h_2 f^{\xi} + h_3\omega_1^{\zeta} - h_4 f^{\zeta} \tag{43d}$$

where ξ and ζ denote two ends of the element and

$$\eta = \frac{x}{l^*} \tag{44}$$

and l^* is the element length of beam; and h_i is cubic Hermitian polynomials as follows:

$$h_1 = 2\eta^3 - 3\eta^2 + 1, \quad h_2 = (\eta^3 - 2\eta^2 + \eta)l^* \\ h_3 = -2\eta^3 + 3\eta^2, \quad h_4 = (\eta^3 - \eta^2)l^* \tag{45a–d}$$

Substituting element displacements in Eq. (43) into Eqs. (4) and (6) and integrating over the element length, the total potential energy of thin-walled composite beam are obtained in a matrix form as

$$\Pi_T = \tfrac{1}{2}\mathbf{U}_e^{\mathrm{T}}(\mathbf{K}_e - \omega^2\mathbf{M}_e)\mathbf{U}_e - \mathbf{U}_e^{\mathrm{T}}\tilde{\mathbf{F}}_e \tag{46}$$

where

$$\mathbf{U}_e = \langle U_x^\xi, U_y^\xi, U_z^\xi, \omega_1^\xi, \omega_2^\xi, \omega_3^\xi, f^\xi, U_x^\zeta, U_y^\zeta, U_z^\zeta, \omega_1^\zeta, \omega_2^\zeta, \omega_3^\zeta, f^\zeta \rangle \tag{47a}$$

$$\tilde{\mathbf{F}}_e = \langle F_1^\xi, F_2^\xi, F_3^\xi, M_1^\xi, M_2^\xi, M_3^\xi, M_\phi^\xi, F_1^\zeta, F_2^\zeta, F_3^\zeta, M_1^\zeta, M_2^\zeta, M_3^\zeta, M_\phi^\zeta \rangle \tag{47b}$$

In Eq. (46), $\mathbf{K}_e$ and $\mathbf{M}_e$ are the element elastic stiffness matrix and the mass matrix in a local coordinate, respectively. In this study, the stiffness matrix is evaluated using the Gauss numerical integration scheme and the assembly of element stiffness matrix for the entire structure based on the coordinate transformation leads to the matrix equation in a global coordinate system.

5. Numerical examples

To demonstrate the efficiency and accuracy of the present study based on the dynamic stiffness matrix, the free vibration analysis of thin-walled composite I-beam with symmetric or arbitrary laminations is performed. For verification, the analytical study by other researchers, the results from available references and the FE analysis using the thin-walled Hermitian beam elements are compared in tables with the current results.

5.1. Simply supported I-beams for comparison

In this example, using the dynamic stiffness matrix, the natural frequencies for the simply supported (S–S) I-beams with symmetric lamination are evaluated. First, we consider the I-beam which has the flange width $b = 60$ cm and the height $h = 60$ cm, as shown in Fig. 3. The beam length l is 1200 cm and the total thicknesses t of flanges and web are assumed to be 3 cm. All constituent flanges and web are assumed to be symmetrically laminated with respect to its midplane. The graphite-epoxy (AS4/3501) is used for the beam with its material properties: $E_1 = 144\,\mathrm{GPa}$, $E_2 = E_3 = 9.65\,\mathrm{GPa}$, $G_{12} = G_{13} = 4.14\,\mathrm{GPa}$, $G_{23} = 3.45\,\mathrm{GPa}$, $v_{12} = v_{13} = 0.3$,

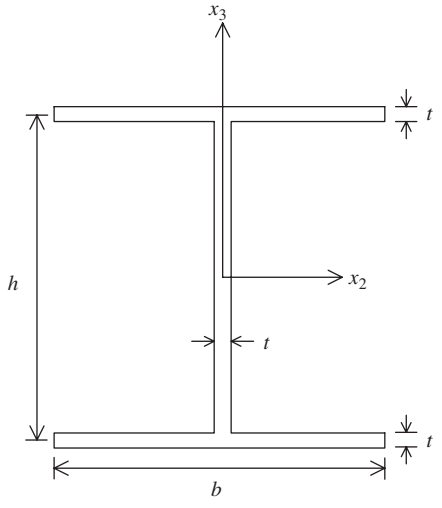

Fig. 3. Cross section of the I-beam.

$\rho = 1389\,\mathrm{kg/m^3}$. Here, subscripts '1' and '2' correspond to directions parallel and perpendicular to fibers, respectively. The considered laminate schemes are [0/0/0/0], [0/90/90/0] and [45/−45/−45/45]. The lowest four torsional natural frequencies for S–S beam obtained from the exact stiffness matrix method (ESMM) are presented and compared with the results of 20 Hermitian beam elements and the analytical solutions by Cortínez and Piovan [14] and Roberts [40] in Table 1. It can be found from Table 1 that the results from this study using only a single element agree well with those from 20 Hermitian beam elements and the analytical solutions. It should be mentioned that the present numerical solutions are exact for the higher vibrational modes as well as the lower ones because the displacement state vector in Eq. (34) satisfies the homogeneous form of the equations of motion. Whereas, a large number of Hermitian beam elements are required to achieve sufficient accuracy for the higher modes.

Next, the S-S I-beam with its length $l = 800\,\mathrm{cm}$ is considered. The flange width b and the height h are 10 and 20 cm, respectively, and the thicknesses t of flanges and web are 1 cm. The following material properties are used: $E_1/E_2 = 40$, $G_{12}/E_2 = 0.6$, $\nu_{12} = 0.25$. The top and bottom flanges are considered as [90/−90] lay-up and the web laminate is assumed to be unidirectional. For convenience, the following non-dimensional natural frequency is used as:

$$\omega^* = \frac{\omega l^2}{h}\sqrt{\frac{\rho}{E_2}} \tag{48}$$

Lee and Kim [2] show that in this case, the results obtained from FE analysis proposed by Lee and Kim [2] and the analytical solutions by Roberts [40] lead discrepancy because of the coupling stiffnesses which are neglected in the analytical analysis. In Table 2, the lowest four non-dimensional natural frequencies from this ESMM, 20 Hermitian beam elements and the FE analysis by Lee and Kim [2] are presented. The excellent agreement between results by this study and 20 Hermitian beam elements and Lee and Kim [2] is evident.

Table 1
Torsional natural frequencies (Hz) of S–S beam with several stacking sequences

Stacking sequence	Formulation	Mode			
		1	2	3	4
[0/0/0/0]	ESMM	16.25	63.24	141.13	249.30
	FE analysis	16.25	63.24	141.14	249.33
	Cortínez and Piovan [14]	16.24	63.35	141.86	251.76
	Analytical solution [40]	16.26	63.41	142.00	252.02
[0/90/90/0]	ESMM	12.23	46.66	103.71	182.93
	FE analysis	12.23	46.66	103.71	182.95
	Cortínez and Piovan [14]	12.19	46.61	103.95	184.21
	Analytical solution [40]	12.24	46.79	104.35	183.93
[45/−45/−45/45]	ESMM	10.96	28.03	53.85	89.05
	FE analysis	10.96	28.03	53.85	89.05
	Cortínez and Piovan [14]	10.98	28.11	54.18	89.99
	Analytical solution [40]	10.96	28.10	54.18	90.02

Table 2
Nondimensional natural frequencies of S–S beam with [90/−90] lay-up in the flanges

Mode	ESMM	FE analysis	Lee and Kim [2]
1	1.192	1.192	1.193
2	4.767	4.767	4.772
3	6.798	6.798	6.780
4	10.724	10.724	10.749

5.2. Symmetrically laminated angle-ply I-beam with various boundary conditions

The symmetric angle-ply I-beam with various fiber directions and boundary conditions are considered. Following dimensions for I-beam are used: both of flange width and height are 5 cm, $t = 0.208$ cm and $l = 200$ cm. The beam is assumed to be made of glass-epoxy with its material properties: $E_1 = 53.78$ GPa, $E_2 = E_3 = 17.93$ GPa, $G_{12} = G_{13} = 8.96$ GPa, $G_{23} = 3.45$ GPa, $v_{12} = v_{13} = 0.25$, $v_{23} = 0.34$, $\rho = 1968.9\,\mathrm{kg/m^3}$. All constituent flanges and web are assumed to be symmetrically laminated angle-ply $[\pm\psi]_{4S}$ with respect to its midplane. Also 16 layers with equal thickness are considered for two flanges and web.

The natural frequencies for S–S beam obtained from ESMM are presented in Table 3 for several fiber orientations. For comparison, the results from 20 Hermitian beam elements and the analytical solutions by Roberts [40] are also presented. The letters Y and Z in Table 3 refer to flexural vibrations with respect to x_2 and x_3 axes, respectively, and the letter T refers to torsional vibration. From Table 3, it can be found that the solutions obtained from the present ESMM coincide with the solutions by Hermitian beam elements and are in an excellent agreement with the analytical solutions.

The 1st and 2nd frequencies for three vibration modes of beams with various boundary conditions are depicted in Figs. 4–7 with respect to fiber angle change. The considered boundary conditions are: the cantilevered (C–F) beam in Fig. 4, the simply (S–S) supported beam in Fig. 5, the clamped–simply (C–S)

Table 3
Natural frequencies (Hz) of S–S I-beam with $[\pm\psi]_{4S}$ angle-ply laminations

Stacking sequence	Formulation	Mode					
		1	2	3	4	5	6
$[0]_{16}$	ESMM	24.194	35.233	45.235	96.726	109.441	180.616
	FE analysis	24.194	35.233	45.235	96.727	109.442	180.616
	Analytical solution [40]	24.198	35.240	45.262	96.792	109.516	181.048
		$Y(1)$	$T(1)$	$Z(1)$	$Y(2)$	$T(2)$	$Z(2)$
$[15/-15]_{4S}$	ESMM	22.997	36.247	42.996	91.940	107.655	171.678
	FE analysis	22.997	36.247	42.996	91.941	107.656	171.679
	Analytical solution [40]	23.001	36.253	43.022	92.003	107.729	172.089
		$Y(1)$	$T(1)$	$Z(1)$	$Y(2)$	$T(2)$	$Z(2)$
$[30/-30]_{4S}$	ESMM	19.816	37.051	37.864	79.225	102.159	147.937
	FE analysis	19.816	37.051	37.864	79.226	102.159	147.938
	Analytical solution [40]	19.820	37.073	37.871	79.279	102.229	148.291
		$Y(1)$	$T(1)$	$Z(1)$	$Y(2)$	$T(2)$	$Z(2)$
$[45/-45]_{4S}$	ESMM	16.487	30.827	37.915	65.916	94.884	123.085
	FE analysis	16.487	30.827	37.915	65.916	94.884	123.086
	Analytical solution [40]	16.490	30.845	37.921	65.961	94.949	123.380
		$Y(1)$	$T(1)$	$Z(1)$	$Y(2)$	$T(2)$	$Z(2)$
$[60/-60]_{4S}$	ESMM	14.666	27.420	35.372	58.633	87.051	109.484
	FE analysis	14.666	27.420	35.372	58.633	87.051	109.485
	Analytical solution [39]	14.668	27.437	35.378	58.673	87.111	109.746
		$Y(1)$	$T(1)$	$Z(1)$	$Y(2)$	$T(2)$	$Z(2)$
$[75/-75]_{4S}$	ESMM	14.077	26.319	31.313	56.278	79.330	105.087
	FE analysis	14.077	26.319	31.313	56.278	79.331	105.088
	Analytical solution [40]	14.079	26.335	31.318	56.316	79.385	105.339
		$Y(1)$	$T(1)$	$Z(1)$	$Y(2)$	$T(2)$	$Z(2)$
$[90/-90]_{4S}$	ESMM	13.970	26.119	29.175	55.850	75.767	104.287
	FE analysis	13.970	26.119	29.175	55.850	75.768	104.288
	Analytical solution [40]	13.972	26.134	29.180	55.880	75.819	104.537
		$Y(1)$	$T(1)$	$Z(1)$	$Y(2)$	$T(2)$	$Z(2)$

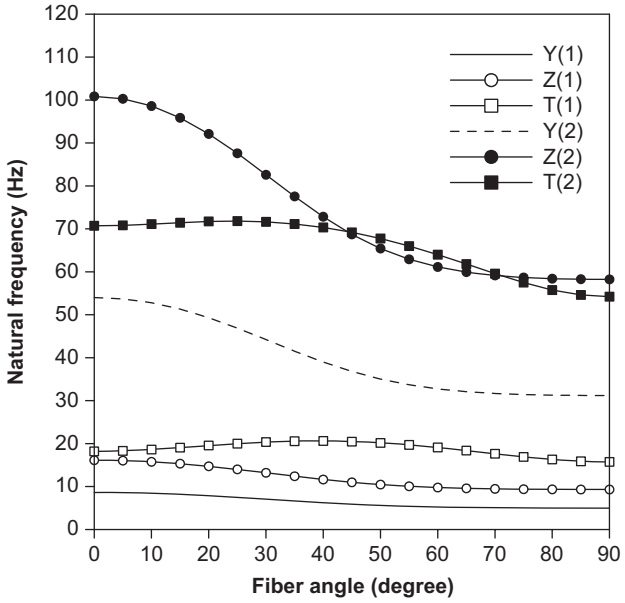

Fig. 4. Variation of the 1st and 2nd frequencies of C–F composite beam with respect to fiber angle change.

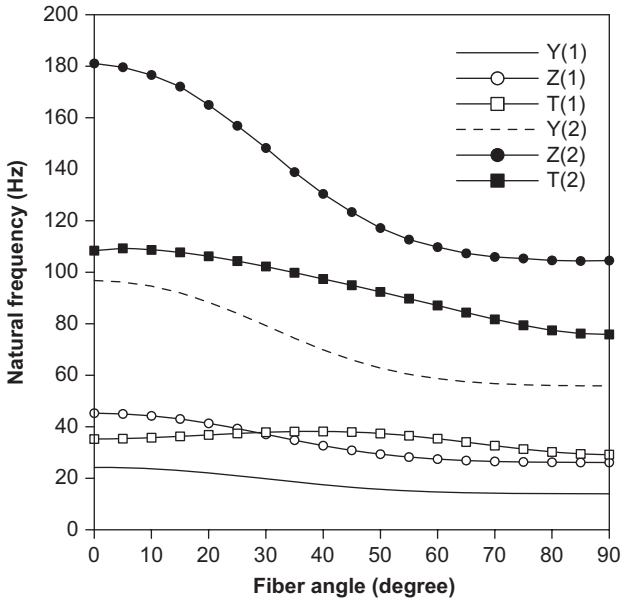

Fig. 5. Variation of the 1st and 2nd frequencies of S–S composite beam with respect to fiber angle change.

supported and the clamped–clamped (C–C) beams in Figs. 6 and 7, respectively. In Figs. 4–7, the number in parenthesis indicates the mode number for associated vibration modes Y, Z, or T.

It is seen from Fig. 4 that for C–F beam, the mode shape corresponding to the lowest natural frequency is the flexural mode in x_2 direction $Y(1)$ and the frequencies $Y(1)$ and $Z(1)$ corresponding to the flexural modes in x_2 and x_3 directions, respectively, decrease as the fiber angle increases. However, in torsional vibration, the stiffness component D_{66} in flanges plays an important role since it affects the torsional rigidity JG, thus, placing the fiber angle at $\psi = 45^\circ$ leads to considerable increase of the torsional frequency for the 1st mode $T(1)$. On the other hand, for the 2nd torsional mode $T(2)$, the frequency is maximum at $\psi = 25^\circ$. Also it can be

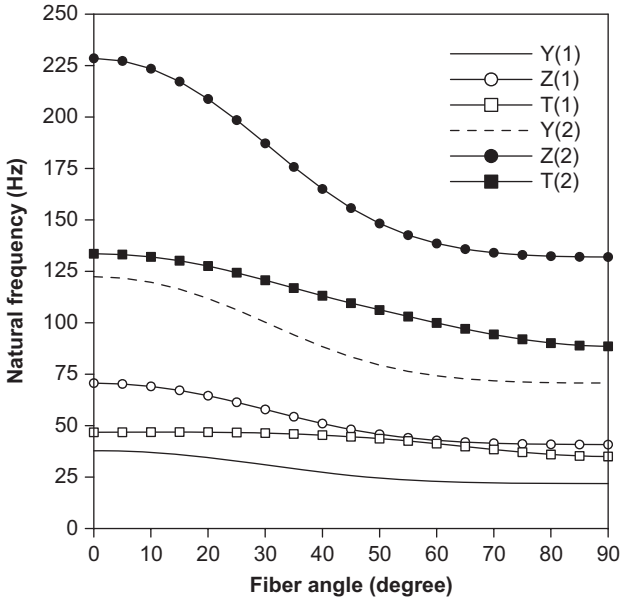

Fig. 6. Variation of the 1st and 2nd frequencies of C–S composite beam with respect to fiber angle change.

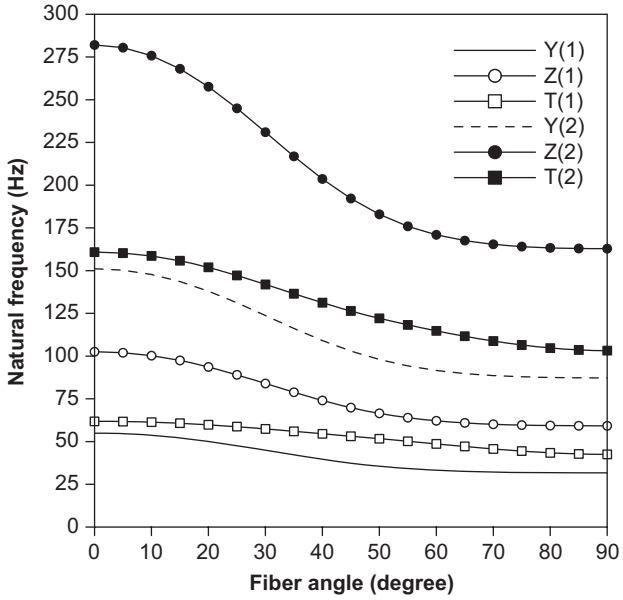

Fig. 7. Variation of the 1st and 2nd frequencies of C–C composite beam with respect to fiber angle change.

observed from Fig. 4 that the 2nd torsional mode $T(2)$ and flexural one in x_3 direction $Z(2)$ change each other at $\psi = 45^\circ$ and 75°. Similar observation can also be found in S–S beam as shown in Fig. 5. That is, the 1st torsional mode and flexural one in x_3 direction change each other at $\psi = 30^\circ$. As a result, the 1st torsional mode, which is above the flexural mode in x_3 direction becomes to be below the flexural one through this mode change phenomenon. Also similar to C–F beam, the 1st tosional frequencies are maximum at $\psi = 45^\circ$ for both of S–S and C–S beams. However, for C–C beam, as can be seen in Fig. 7, the 1st and 2nd torsional modes including the flexural modes in x_2 and x_3 directions decrease as the fiber angle increases.

To investigate the effects of increase of the modulus on vibration characteristics of composite beams with various boundary conditions, when E_1 is increased into $10E_1$, the 1st flexural and torsional natural frequencies

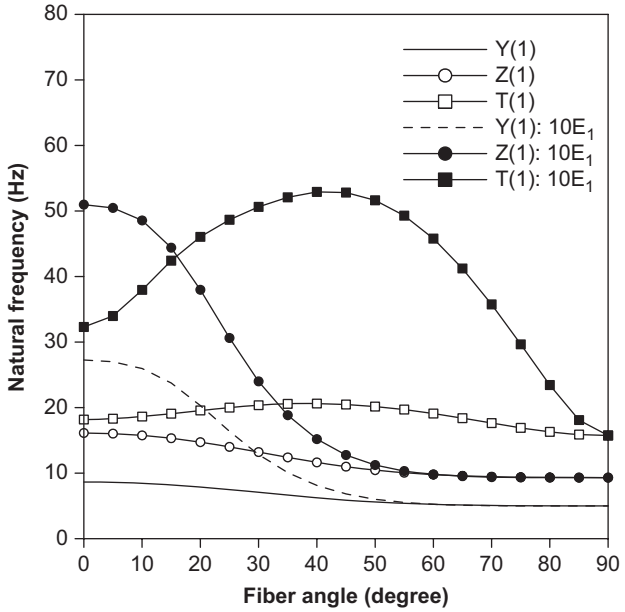

Fig. 8. Effects of increase of the modulus on the 1st frequencies of C–F composite beam with respect to fiber angle change.

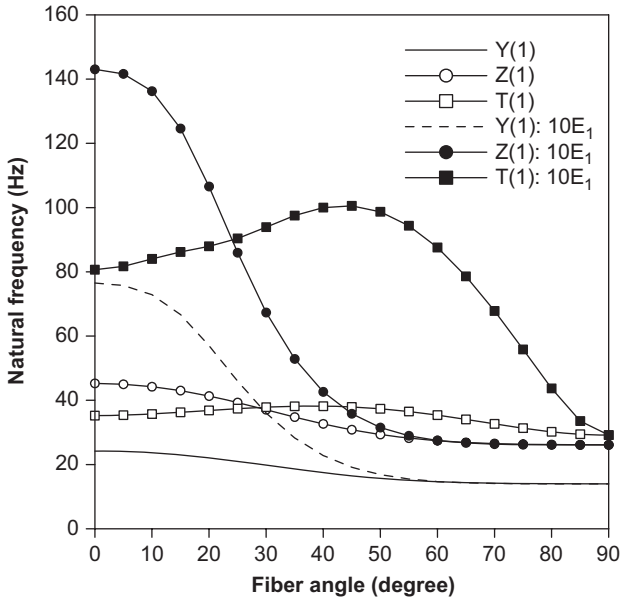

Fig. 9. Effects of increase of the modulus on the 1st frequencies of S–S composite beam with respect to fiber angle change.

are illustrated in Figs. 8–11. It can be observed from Fig. 8 that for C–F beam with $10E_1$, the mode change phenomenon between the torsional mode and the flexural mode in x_3 direction occurs at $\psi = 16^\circ$. Also the fiber angle at which the fundamental mode change occurs increases as the end boundary of beam is restrained more (i.e. $\psi = 24^\circ$ for S–S beam, $\psi = 30^\circ$ and 35° for C–S and C–C beams, respectively). Furthermore, Figs. 12 and 13 show the increase ratio of the 1st flexural and torsional natural frequencies, respectively, due to increase of the modulus. It is interesting to observe from Fig. 12 that as the fiber angle increases, the increase ratios for the flexural modes corresponding to x_2 and x_3 directions decrease monotonically and both of the flexural frequencies are unaffected by increase of the modulus after $\psi = 60^\circ$ regardless of boundary

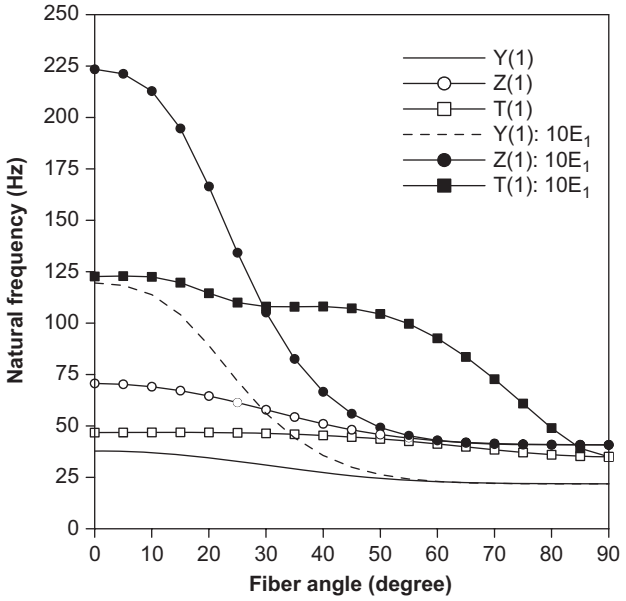

Fig. 10. Effects of increase of the modulus on the 1st frequencies of C–S composite beam with respect to fiber angle change.

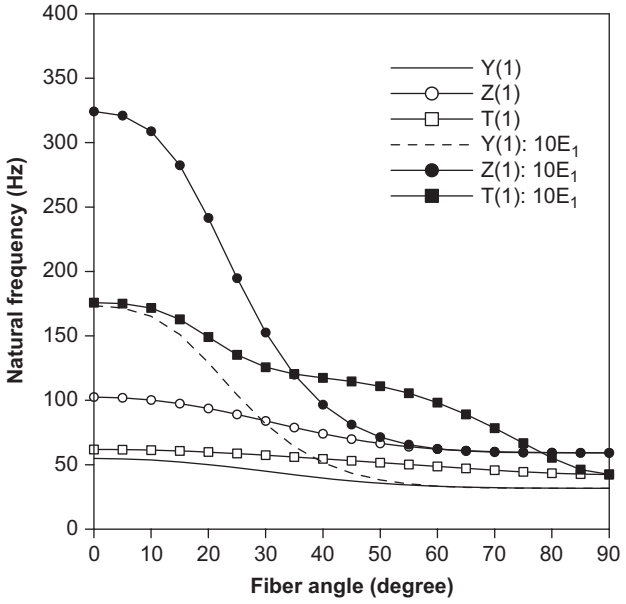

Fig. 11. Effects of increase of the modulus on the 1st frequencies of C–C composite beam with respect to fiber angle change.

conditions. This is because of decrease of the flexural rigidities I_2 and I_3. Whereas, the increase ratios for the torsional frequencies reach its maximum at $\psi = 45^\circ$ for C–F and S–S beams and at $\psi = 0^\circ$ for C–S and C–C beams.

Next, the effect of bending–twisting coupling stiffness D_{26} on the torsional vibrational behavior of the composite beam is investigated. The angle-ply lamination $[45/-45]_{NS}$ with different numbers of N is considered while maintaining the total thickness as constant. As N increases, the bending-twisting coupling stiffness D_{26} which affects the torsional constant JG becomes negligible as presented in the 2nd column

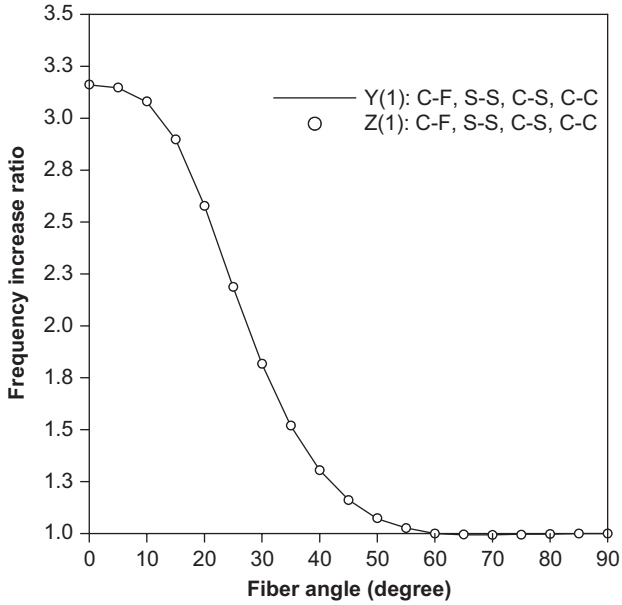

Fig. 12. Increase ratio of the 1st flexural natural frequencies of composite beam due to increase of the modulus.

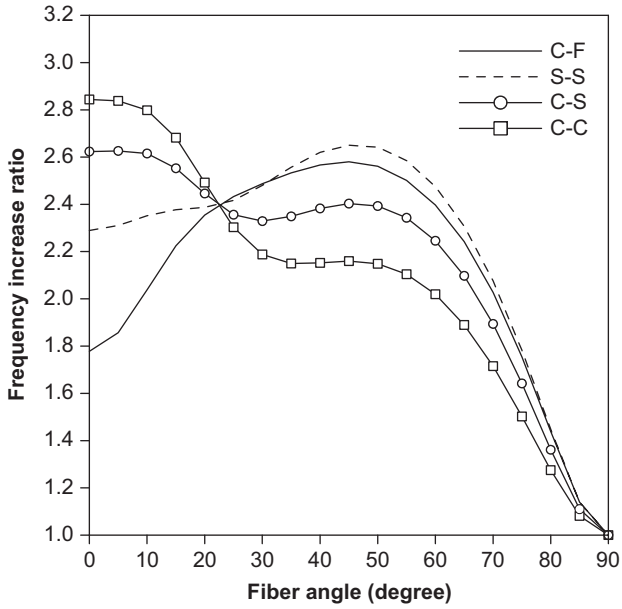

Fig. 13. Increase ratio of the 1st torsional natural frequencies of composite beam due to increase of the modulus.

(D_{26}/D_{22}) of Table 4. It can be seen from Table 4 that the 1st torsional natural frequencies decrease slightly for four beams with relatively greater value of coupling stiffness D_{26}.

5.3. Arbitrarily laminated clamped I-beam

In our final example, we intend to evaluate exactly the extensionally–flexurally–torsionally coupled natural frequencies of an arbitrarily laminated I-beam. The dimension and the material properties of beam are the same as the previous example and the C–C boundary condition is considered. The flanges and web of the beam

Table 4
The 1st torsional natural frequencies (Hz) of beams with $[45/-45]_{NS}$ lamination and with various boundary conditions

N	D_{26}/D_{22}	C–F	S–S	C–S	C–C
1	0.232	19.676	36.442	43.218	51.841
2	0.116	20.315	37.625	44.324	52.845
4	0.058	20.471	37.915	44.594	53.092
8	0.029	20.510	37.987	44.660	53.154

Table 5
Coupled natural frequencies (Hz) of C–C beam with [0/30/60/90] lamination

Mode	FE analysis					ESMM
	4	6	8	10	20	
1	42.457	42.412	42.404	42.402	42.401	42.400
2	51.492	51.435	51.426	51.423	51.421	51.421
3	79.544	79.460	79.445	79.441	79.439	79.439
4	117.890	117.039	116.884	116.841	116.812	116.810
5	130.547	129.692	129.542	129.501	129.474	129.472
6	220.546	218.957	218.666	218.585	218.532	218.528
7	233.654	230.423	229.327	229.011	228.799	228.785
8	247.696	244.115	243.049	242.746	242.545	242.532
9	436.053	384.308	380.073	378.715	377.783	377.719
10	441.420	398.100	393.911	392.590	391.691	391.629

are assumed to have four layers of [0/30/60/90] lamination with equal ply thicknesses. In this case, all coupling stiffnesses are non-zero except for S_2. The lowest ten spatially coupled natural frequencies for the beam obtained from ESMM are presented in Table 5 and compared with the results using various numbers of Hermitian beam elements. From Table 5, it is observed that the coupled frequencies from ESMM using only a single element are in an excellent agreement with the results obtained by using as many as 20 Hermitian beam elements. It should be noted that the natural frequencies from the present numerical method are exact for the higher vibrational modes as well as for the lower ones in the sense that the value of natural frequencies satisfies the solution of a simultaneous ordinary differential equations in (10), (15) to (17) exactly. Still, a large number of Hermitian beam elements needs to be used to obtain sufficiently accurate results especially for the higher vibration modes.

6. Conclusion

This study is the first attempt to deal with the exact natural frequencies of thin-walled composite I-beam with arbitrary lamination. For this, the exact dynamic stiffness matrix for the spatially coupled free vibration analysis of thin-walled composite I-beam with symmetric and arbitrary laminations is presented. The higher-order simultaneous ordinary differential equations of the arbitrarily laminated thin-walled beam are first derived and transformed into the first-order differential equations by introducing 14 displacement parameters. Then exact solutions of displacement parameters are obtained using a generalized linear eigenproblem having complex eigenvalues. Finally the dynamic element stiffness matrix of the harmonically vibrating composite beam is determined using member force–displacement relationships. Furthermore, the FE model using the Hermitian beam elements including the restrained warping is developed.

Through numerical examples, it is demonstrated that results by present method using the dynamic element stiffness matrix have shown to be in an excellent agreement with the analytical solutions, the results by available references and those from a large number of Hermitian beam elements. Also the mode change phenomenon, the effect of increase of the modulus and the effect of bending–twisting coupling stiffness on the

free vibration characteristics of beams with various boundary conditions are investigated for angle-ply laminates with different fiber orientations.

Consequently it is believed that the present numerical procedure is general enough to provide a systematic tool for not only the numerical evaluation of exact dynamic element stiffness matrix of thin-walled composite beam but also general solutions of simultaneous ordinary differential equations of the higher order. Furthermore, this exact composite beam element eliminates discretization errors and is capable of predicting an infinite number of natural frequencies of composite beams by means of a finite number of coordinates.

Acknowledgements

This work is a part of a research project supported by Korea Ministry of Construction & Transportation through Korea Bridge Design & Engineering Research Center at Seoul National University. The authors wish to express their gratitude for the financial support.

Appendix A. The beam stress resultants which are equivalent to plate stress resultants

$$F_1 = \int_C N_x \, \mathrm{d}s \tag{A.1}$$

$$F_2 = \int_C \left(x_2 \frac{\partial N_x}{\partial x_1} - \frac{\partial M_x}{\partial x_1} \sin \psi \right) \mathrm{d}s - m_3 = -\frac{\partial M_3}{\partial x_1} - m_3 \tag{A.2}$$

$$F_3 = \int_C \left(x_3 \frac{\partial N_x}{\partial x_1} + \frac{\partial M_x}{\partial x_1} \cos \psi \right) \mathrm{d}s + m_2 = \frac{\partial M_2}{\partial x_1} + m_2 \tag{A.3}$$

$$M_1 = T_\omega + T_s = \int_C \left(\phi \frac{\partial N_x}{\partial x_1} + q \frac{\partial M_x}{\partial x_1} \right) \mathrm{d}s - m_\omega - \int_C (M_{sx} + M_{xs}) \, \mathrm{d}s \tag{A.4}$$

$$M_2 = \int_C (N_x x_3 + M_x \cos \psi) \, \mathrm{d}s \tag{A.5}$$

$$M_3 = -\int_C (N_x x_2 - M_x \sin \psi) \, \mathrm{d}s \tag{A.6}$$

$$M_\phi = \int_C (N_x \omega + M_x q) \, \mathrm{d}s \tag{A.7}$$

where m_1, m_2, m_3, and m_ω are the moment distributions.

Appendix B. The detailed expression of the sectional quantities

$$A = \int_C A_{11}^* \, \mathrm{d}s \tag{B.1}$$

$$S_2 = \int_C (A_{11}^* x_3 + B_{11}^* \cos \psi) \, \mathrm{d}s \tag{B.2}$$

$$S_3 = \int_C (A_{11}^* x_2 - B_{11}^* \sin \psi) \, \mathrm{d}s \tag{B.3}$$

$$S_w = \int_C (A_{11}^* \phi + B_{11}^* q) \, \mathrm{d}s \tag{B.4}$$

$$S_\phi = -2\int_C B_{16}^* \,\mathrm{d}s \tag{B.5}$$

$$H_c = 2\int_C (B_{16}^* x_3 + D_{16}^* \cos\psi)\,\mathrm{d}s \tag{B.6}$$

$$H_s = -2\int_C (B_{16}^* x_2 - D_{16}^* \sin\psi)\,\mathrm{d}s \tag{B.7}$$

$$H_q = 2\int_C (B_{16}^* \phi + D_{16}^* q)\,\mathrm{d}s \tag{B.8}$$

$$I_2 = \int_C (A_{11}^* x_3^2 + 2B_{11}^* x_3 \cos\psi + D_{11}^* \cos^2\psi)\,\mathrm{d}s \tag{B.9}$$

$$I_3 = \int_C (A_{11}^* x_2^2 - 2B_{11}^* x_2 \sin\psi + D_{11}^* \sin^2\psi)\,\mathrm{d}s \tag{B.10}$$

$$I_{23} = \int_C \{A_{11}^* x_2 x_3 + B_{11}^*(x_2 \cos\psi - x_3 \sin\psi) - D_{11}^* \sin\psi \cos\psi\}\,\mathrm{d}s \tag{B.11}$$

$$I_\phi = \int_C (A_{11}^* \phi^2 + 2B_{11}^* q\phi + D_{11}^* q^2)\,\mathrm{d}s \tag{B.12}$$

$$I_{\phi 2} = \int_C \{A_{11}^* x_3 \phi + B_{11}^*(x_3 q + \phi \cos\psi) + D_{11}^* q \cos\psi\}\,\mathrm{d}s \tag{B.13}$$

$$I_{\phi 3} = \int_C \{A_{11}^* x_2 \phi + B_{11}^*(x_2 q - \phi \sin\psi) - D_{11}^* q \sin\psi\}\,\mathrm{d}s \tag{B.14}$$

$$JG = 4\int_C D_{66}^* \,\mathrm{d}s \tag{B.15}$$

where

$$A_{11}^* = A_{11} - \frac{A_{12}^2 D_{22} - 2A_{12}B_{12}B_{22} + A_{22}B_{12}^2}{A_{22}D_{22} - B_{22}^2} \tag{B.16}$$

$$A_{16}^* = A_{16} - \frac{A_{12}A_{26}D_{22} - A_{12}B_{22}B_{26} - A_{26}B_{12}B_{22} + A_{22}B_{12}B_{26}}{A_{22}D_{22} - B_{22}^2} \tag{B.17}$$

$$B_{11}^* = B_{11} - \frac{A_{12}B_{12}D_{22} - A_{12}B_{22}D_{12} - B_{12}^2 B_{22} + A_{22}B_{12}D_{12}}{A_{22}D_{22} - B_{22}^2} \tag{B.18}$$

$$B_{16}^* = B_{16} - \frac{A_{12}B_{26}D_{22} - A_{12}B_{22}D_{26} - B_{12}B_{22}B_{26} + A_{22}B_{12}D_{26}}{A_{22}D_{22} - B_{22}^2} \tag{B.19}$$

$$\tilde{B}_{16}^* = B_{16} - \frac{A_{26}B_{12}D_{22} - A_{26}B_{22}D_{12} - B_{12}B_{22}B_{26} + A_{22}B_{26}D_{12}}{A_{22}D_{22} - B_{22}^2} \tag{B.20}$$

$$B_{66}^* = B_{66} - \frac{A_{26}B_{26}D_{22} - A_{26}B_{22}D_{26} - B_{22}B_{26}^2 + A_{22}B_{26}D_{26}}{A_{22}D_{22} - B_{22}^2} \tag{B.21}$$

$$D_{11}^{*} = D_{11} - \frac{B_{12}^2 D_{22} - 2B_{12}B_{22}D_{12} + A_{22}D_{12}^2}{A_{22}D_{22} - B_{22}^2} \tag{B.22}$$

$$D_{16}^{*} = D_{16} - \frac{B_{12}B_{26}D_{22} - B_{12}B_{22}D_{26} - B_{22}B_{26}D_{12} + A_{22}D_{12}D_{26}}{A_{22}D_{22} - B_{22}^2} \tag{B.23}$$

$$D_{66}^{*} = D_{66} - \frac{B_{26}^2 D_{22} - 2B_{22}B_{26}D_{26} + A_{22}D_{26}^2}{A_{22}D_{22} - B_{22}^2} \tag{B.24}$$

Appendix C. The detailed components of matrices $\mathbf{A}_n$, $\mathbf{B}_n$ and $\mathbf{S}$

(1) Components of matrix $\mathbf{A}_n$

$$\mathbf{A}_n = \begin{bmatrix}
1 & \cdot & \cdot & \cdot & \cdot & \cdot & \cdot & \cdot & \cdot & \cdot & \cdot & \cdot & \cdot & \cdot \\
\cdot & A & \cdot & \cdot & \cdot & \cdot & \cdot & \cdot & \cdot & \cdot & \cdot & \cdot & \cdot & \cdot \\
\cdot & \cdot & 1 & \cdot & \cdot & \cdot & \cdot & \cdot & \cdot & \cdot & \cdot & \cdot & \cdot & \cdot \\
\cdot & \cdot & \cdot & 1 & \cdot & \cdot & \cdot & \cdot & \cdot & \cdot & \cdot & \cdot & \cdot & \cdot \\
\cdot & \cdot & \cdot & \cdot & 1 & \cdot & \cdot & \cdot & \cdot & \cdot & \cdot & \cdot & \cdot & \cdot \\
\cdot & \cdot & \cdot & \cdot & \cdot & \tilde{I}_3 & \cdot & \cdot & \cdot & \tilde{I}_{23} & \cdot & \cdot & \cdot & \tilde{I}_{\phi 3} \\
\cdot & \cdot & \cdot & \cdot & \cdot & \cdot & 1 & \cdot & \cdot & \cdot & \cdot & \cdot & \cdot & \cdot \\
\cdot & \cdot & \cdot & \cdot & \cdot & \cdot & \cdot & 1 & \cdot & \cdot & \cdot & \cdot & \cdot & \cdot \\
\cdot & \cdot & \cdot & \cdot & \cdot & \cdot & \cdot & \cdot & 1 & \cdot & \cdot & \cdot & \cdot & \cdot \\
\cdot & \cdot & \cdot & \cdot & \cdot & \tilde{I}_{23} & \cdot & \cdot & \cdot & \tilde{I}_2 & \cdot & \cdot & \cdot & \tilde{I}_{\phi 2} \\
\cdot & \cdot & \cdot & \cdot & \cdot & \cdot & \cdot & \cdot & \cdot & \cdot & 1 & \cdot & \cdot & \cdot \\
\cdot & \cdot & \cdot & \cdot & \cdot & \cdot & \cdot & \cdot & \cdot & \cdot & \cdot & 1 & \cdot & \cdot \\
\cdot & \cdot & \cdot & \cdot & \cdot & \cdot & \cdot & \cdot & \cdot & \cdot & \cdot & \cdot & 1 & \cdot \\
\cdot & -S_{\phi} & \cdot & \cdot & \cdot & \tilde{I}_{\phi 3} & \cdot & \cdot & \cdot & \tilde{I}_{\phi 2} & \cdot & \cdot & \cdot & \tilde{I}_{\phi}
\end{bmatrix} \tag{C.1}$$

(2) Components of matrix $\mathbf{B}_n$

$$\mathbf{B}_n = \begin{bmatrix}
\cdot & b_1 & \cdot & \cdot & \cdot & \cdot & \cdot & \cdot & \cdot & \cdot & \cdot & \cdot & \cdot & \cdot \\
b_2 & \cdot & \cdot & \cdot & \cdot & b_3 & \cdot & \cdot & \cdot & b_4 & \cdot & \cdot & b_5 & b_6 \\
\cdot & \cdot & \cdot & b_1 & \cdot & \cdot & \cdot & \cdot & \cdot & \cdot & \cdot & \cdot & \cdot & \cdot \\
\cdot & \cdot & \cdot & \cdot & b_1 & \cdot & \cdot & \cdot & \cdot & \cdot & \cdot & \cdot & \cdot & \cdot \\
\cdot & \cdot & \cdot & \cdot & \cdot & b_1 & \cdot & \cdot & \cdot & \cdot & \cdot & \cdot & \cdot & \cdot \\
\cdot & b_7 & -b_2 & \cdot & b_8 & \cdot & \cdot & \cdot & b_9 & \cdot & b_{10} & \cdot & b_{11} & b_{12} \\
\cdot & \cdot & \cdot & \cdot & \cdot & \cdot & \cdot & b_1 & \cdot & \cdot & \cdot & \cdot & \cdot & \cdot \\
\cdot & \cdot & \cdot & \cdot & \cdot & \cdot & \cdot & \cdot & b_1 & \cdot & \cdot & \cdot & \cdot & \cdot \\
\cdot & \cdot & \cdot & \cdot & \cdot & \cdot & \cdot & \cdot & \cdot & b_1 & \cdot & \cdot & \cdot & \cdot \\
\cdot & b_{13} & \cdot & \cdot & b_9 & \cdot & -b_2 & \cdot & b_{14} & \cdot & b_{15} & \cdot & b_{16} & b_{17} \\
\cdot & \cdot & \cdot & \cdot & \cdot & \cdot & \cdot & \cdot & \cdot & \cdot & \cdot & b_1 & \cdot & \cdot \\
\cdot & \cdot & \cdot & \cdot & \cdot & \cdot & \cdot & \cdot & \cdot & \cdot & \cdot & \cdot & b_1 & \cdot \\
\cdot & \cdot & \cdot & \cdot & \cdot & \cdot & \cdot & \cdot & \cdot & \cdot & \cdot & \cdot & \cdot & b_1 \\
\cdot & b_{18} & b_{10} & \cdot & b_{11} & b_{19} & b_{15} & \cdot & b_{16} & b_{20} & b_{21} & \cdot & b_{22} & b_{23}
\end{bmatrix} \tag{C.2}$$

where

$$b_1 = 1, \quad b_2 = -\rho\omega^2 A^*, \quad b_3 = S_3, \quad b_4 = S_2, \quad b_5 = -S_\phi, \quad b_6 = S_w, \quad b_7 = -\rho\omega^2 A^* S_3/A,$$
$$b_8 = -\rho\omega^2 I_3^*, \quad b_9 = -\rho\omega^2 I_{23}^*, \quad b_{10} = -\rho\omega^2 A^*(z - z_P), \quad b_{11} = -\rho\omega^2 I_{\phi 3}^*,$$
$$b_{12} = \tilde{H}_s, \quad b_{13} = -\rho\omega^2 A^* S_2/A, \quad b_{14} = -\rho\omega^2 I_2^*, \quad b_{15} = \rho\omega^2 A^*(y - y_P),$$
$$b_{16} = -\rho\omega^2 I_{\phi 2}^*, \quad b_{17} = -\tilde{H}_c, \quad b_{18} = -\rho\omega^2 A^* S_w/A, \quad b_{19} = -H_s, \quad b_{20} = H_c$$
$$b_{21} = \rho\omega^2 I_o^*, \quad b_{22} = JG - \rho\omega^2 I_\phi^*, \quad b_{23} = -S_\phi S_w/A \tag{C.3}$$

(3) Components of matrix **S**

$$\mathbf{S} = \begin{bmatrix}
\cdot & A & \cdot & \cdot & -S_3 & \cdot & \cdot & \cdot & -S_2 & \cdot & \cdot & S_\phi & -S_w & \cdot \\
-\rho\omega^2 \frac{A*}{A} S_3 & \cdot & \cdot & -\rho\omega^2 I_3^* & \cdot & -\tilde{I}_3 & \cdot & -\rho\omega^2 I_{23}^* & \cdot & -\tilde{I}_{23} & \cdot & -\rho\omega^2 I_{\phi 3}^* & \tilde{H}_s & -\tilde{I}_{\phi 3} \\
-\rho\omega^2 \frac{A*}{A} S_2 & \cdot & \cdot & -\rho\omega^2 I_{23}^* & \cdot & -\tilde{I}_{23} & \cdot & -\rho\omega^2 I_2^* & \cdot & -\tilde{I}_2 & \cdot & -\rho\omega^2 I_{\phi 2}^* & -\tilde{H}_c & -\tilde{I}_{\phi 2} \\
-\rho\omega^2 \frac{A*}{A} S_w & S_\phi & \cdot & -\rho\omega^2 I_{\phi 3}^* & -H_s & -\tilde{I}_{\phi 3} & \cdot & -\rho\omega^2 I_{\phi 2}^* & H_c & -\tilde{I}_{\phi 2} & \cdot & JG - \rho\omega^2 I_\phi^* & -\frac{S_\phi S_w}{A} & -\tilde{I}_\phi \\
\cdot & S_2 & \cdot & \cdot & -I_{23} & \cdot & \cdot & \cdot & -I_2 & \cdot & \cdot & -H_c & -I_{\phi 2} & \cdot \\
\cdot & -S_3 & \cdot & \cdot & I_3 & \cdot & \cdot & \cdot & I_{23} & \cdot & \cdot & -H_s & I_{\phi 3} & \cdot \\
\cdot & S_w & \cdot & \cdot & -I_{\phi 3} & \cdot & \cdot & \cdot & -I_{\phi 2} & \cdot & \cdot & -H_q & -I_\phi & \cdot
\end{bmatrix} \tag{C.4}$$

References

[1] M.T. Piovan, V.H. Cortínez, Mechanics of shear deformable thin-walled beams made of composite materials, *Thin-Walled Structures* 45 (2007) 37–62.

[2] J. Lee, S.E. Kim, Free vibration of thin-walled composite beams with I-shaped cross-sections, *Composite Structures* 55 (2002) 205–215.

[3] S.R. Marur, T. Kant, Free vibration analysis of fiber reinforced composite beams using higher order theories and finite element modeling, *Journal of Sound and Vibration* 194 (1996) 337–351.

[4] K. Chandrashekhara, K.M. Bangera, Free vibration of composite beams suing a refined shear flexible beam element, *Computers and Structures* 43 (1992) 719–727.

[5] G. Shi, K.Y. Lam, Finite element vibration analysis of composite beams based on higher-order beam theory, *Journal of Sound and Vibration* 219 (1999) 707–721.

[6] P.R. Heyliger, J.N. Reddy, A higher order beam finite element for bending and vibration problems, *Journal of Sound and Vibration* 126 (1988) 309–326.

[7] D.Kr. Maiti, P.K. Sinha, Bending and free vibration analysis of shear deformable laminated composite beams by finite element method, *Composite Structures* 29 (1994) 421–431.

[8] S.M. Rao, N. Ganesan, Dynamic response of non-uniform composite beams, *Journal of Sound and Vibration* 200 (1997) 563–577.

[9] M.S. Nabi, N. Ganesan, Generalized element for the free vibration analysis of composite beams, *Computers and Structures* 51 (1994) 607–610.

[10] D.H. Hodges, A.R. Atilgan, M.V. Fulton, L.W. Rehfield, Free vibration analysis of composite beams, *Journal of the American Helicopter Society* 36 (1991) 36–47.

[11] A.D. Stemple, S.W. Lee, Large deflection static and dynamic finite element analysis of composite beams with arbitrary cross-sectional warping, AIAA Paper No. 89-2363-CP, *Proceedings of the 30th AIAA/ASME/AHS/ACS Structures, Structural Dynamics and Materials Conferences*, Mobile, AL, April 1989, pp. 1788–1798.

[12] X.X. Wu, C.T. Sun, Vibration analysis of laminated composite thin-walled beams using finite elements, *AIAA Journal* 29 (1990) 736–742.

[13] R.K. Gupta, A. Venkatesh, K.P. Rao, Finite element analysis of laminated anisotropic thin-walled open-section beams, *Composite Structures* 3 (1985) 19–31.

[14] V.H. Cortínez, M.T. Piovan, Vibration and buckling of composite thin-walled beams with shear deformability, *Journal of Sound and Vibration* 258 (2002) 701–723.

[15] L.P. Kollár, Flexural–torsional vibration of open section composite beams with shear deformation, *International Journal of Solids and Structures* 38 (2001) 7543–7558.

[16] H. Matsunaga, Vibration and buckling of multilayered composite beams according to higher order deformation theory, *Journal of Sound and Vibration* 246 (2001) 47–62.

[17] O. Song, L. Librescu, Anisotropy and structural coupling on vibration and instability of spinning thin-walled beams, *Journal of Sound and Vibration* 204 (1997) 477–494.

[18] O. Song, L. Librescu, Free vibration of anisotropic composite thin-walled beams of closed cross-section contour, *Journal of Sound and Vibration* 167 (1993) 129–147.
[19] S.J. Song, A.M. Waas, Effects of shear deformation on buckling and free vibration of laminated composite beams, *Composite Structures* 37 (1997) 33–43.
[20] Y. Teboub, P. hajela, Free vibration of generally layered composite beams using symbolic computations, *Composite Structures* 33 (1995) 123–134.
[21] S.H. Farghaly, R.M. Gadelrab, Free vibration of a stepped composite Timoshenko cantilever beam, *Journal of Sound and Vibration* 187 (1995) 886–896.
[22] O. Rand, Free vibration of thin-walled composite blades, *Composite Structures* 28 (1994) 169–180.
[23] K. Chandrashekhara, K. Krishnamurthy, S. Roy, Free vibration of composite beams including rotary inertia and shear deformation, *Composite Structures* 14 (1990) 269–279.
[24] J.R. Vinson, R.L. Sierakowski, *The Behavior of Structures Composed of Composite Materials*, Martinus Nijhoff, Dordrecht, The Netherlands, 1986.
[25] V. Yildirim, E. Sancaktar, E. Kiral, Free vibration analysis of symmetric cross-ply laminated composite beams with the help of the transfer matrix approach, *Communications in Numerical Methods in Engineering* 15 (1999) 651–660.
[26] V. Yildirim, E. Kiral, Investigation of the rotary inertia and shear deformation effects on the out-of-plane bending and torsional natural frequencies of laminated beams, *Composite Structures* 49 (2000) 313–320.
[27] A.A. Khdeir, J.N. Reddy, Free vibration of cross-ply laminated beams with arbitrary boundary conditions, *International Journal of Engineering Sciences* 32 (1994) 1971–1980.
[28] J.R. Banerjee, F.W. Williams, Free vibration of composite beams—an exact method using symbolic computation, *Journal of Aircraft* 32 (1995) 636–642.
[29] J.R. Banerjee, F.W. Williams, Exact dynamic stiffness matrix for composite Timoshenko beams with applications, *Journal of Sound and Vibration* 194 (1996) 573–585.
[30] J.R. Banerjee, Free vibration of axially loaded composite Timoshenko beams using the dynamic stiffness matrix method, *Computers and Structures* 69 (1998) 197–208.
[31] J.R. Banerjee, Frequency equation and mode shape formulae for composite Timoshenko beams, *Composite Structures* 51 (2001) 381–388.
[32] H. Abramovich, Shear deformation and rotary inertia effects of vibrating composite beams, *Composite Structures* 20 (1992) 165–173.
[33] H. Abramovich, A. Livshits, Free vibrations of non-symmetric cross-ply laminated composite beams, *Journal of Sound and Vibration* 176 (1994) 597–612.
[34] H. Abramovich, M. Eisenberger, O. Shulepov, Vibrations and buckling of cross-ply nonsymmetric laminated composite beams, *AIAA Journal* 34 (1996) 1064–1069.
[35] M. Eisenberger, H. Abramovich, O. Shulepov, Dynamic stiffness analysis of laminated beams using a first-order shear deformation theory, *Composite Structures* 31 (1995) 265–271.
[36] A. Gjelsvik, *The Theory of Thin-Walled Bars*, Wiley, New York, 1981.
[37] R.M. Jones, *Mechanics of Composite Material*, McGraw-Hill, New York, 1975.
[38] D.K. Shin, N.I. Kim, K.Y. Kim, Exact stiffness matrix of mono-symmetric composite I-beam with arbitrary lamination, *Composite Structures* 79 (2007) 467–480.
[39] Microsoft IMSL Library, Microsoft Corporation, 1995.
[40] T.M. Roberts, Natural frequencies of thin-walled bars of open cross section, *Journal of Structural Engineering* 113 (1987) 1584–1593.